Published in final edited form as:
Biol Chem. 2011 August ; 392(8-9): 699–712. doi:10.1515/BC.2011.091.

Genetic interactions with mutations affecting septin assembly reveal ESeRT functions in budding yeast cytokinesis*

Michael A. McMurray[1], **Christopher J. Stefan**[2], **Megan Wemmer**[3], **Greg Odorizzi**[3], **Scott D. Emr**[2], and **Jeremy Thomer**[1,**]

[1]Division of Biochemistry and Molecular Biology, Department of Molecular and Cell Biology, University of California, Berkeley, CA 94720-3202, USA

[2]Weill Institute for Cell and Molecular Biology, Cornell University, Ithaca, NY 14853-7202, USA

[3]Department of Molecular, Cellular, and Developmental Biology, University of Colorado, Boulder, CO 80309-0347, USA

Abstract

Membrane trafficking via targeted exocytosis to the *Saccharomyces cerevisiae* bud neck provides new membrane and membrane-associated factors that are critical for cytokinesis. It remains unknown whether yeast plasma membrane abscission, the final step of cytokinesis, occurs spontaneously following extensive vesicle fusion, as in plant cells, or requires dedicated membrane fission machinery, as in cultured mammalian cells. Components of the endosomal sorting complexes required for transport (ESCRT) pathway, or close relatives thereof, appear to participate in cytokinetic abscission in various cell types, but roles in cell division had not been documented in budding yeast, where ESCRTs were first characterized. By contrast, the septin family of filament-forming cytoskeletal proteins were first identified by their requirement for yeast cell division. We show here that mutations in ESCRT-encoding genes exacerbate the cytokinesis defects of *cla4Δ* or *elm1Δ* mutants, in which septin assembly is perturbed at an early stage in cell division, and alleviate phenotypes of cells carrying temperature-sensitive alleles of a septin-encoding gene, *CDC10*. Elevated chitin synthase II (Chs2) levels coupled with aberrant morphogenesis and chitin deposition in *elm1Δ* cells carrying ESCRT mutations suggest that ESCRTs normally enhance the efficiency of cell division by promoting timely endocytic turnover of key cytokinetic enzymes.

Keywords

abscission; cell division; endocytosis; exocytosis; septation; suppression

Introduction

Cell division requires the resolution of a single continuous plasma membrane into two. In most eukaryotes, the two sides of the plasma membrane are brought in close proximity by an actomyosin-based contractile ring that guides ingression of a cleavage furrow. However, the

*Electronic supplementary material to this article with the DOI 10.1515/BC.2011.091SUP is available from the journals online content site at www.reference-global.com/toc/bchm/392/8-9.

**Corresponding author jthomer@berkeley.edu.

Web sites *Saccharomyces cerevisiae* Morphology Database (SCMD), http://yeast.gi.k.u-tokyo.ac.jp/. *Saccharomyces* Genome Database (SGD)™, http://www.yeastgenome.org/.

mechanism by which plasma membrane abscission ultimately occurs remains obscure (Guizetti and Gerlich, 2010). Delivery of Golgi-derived or recycled endosomal vesicles to the site of plasma membrane abscission plays an important yet poorly characterized role, but the exocyst complex, which targets the docking of exocytic vesicles, seems to be involved (He and Guo, 2009). In many eukaryotes, efficient execution of the abscission step also requires certain members of the septin family of GTP-binding proteins, known to polymerize into membrane-associated filaments (Kinoshita and Noda, 2001). Prior to ingression, septin assemblies localize at the incipient cleavage site and help recruit components of the contractile ring. Additionally, septin filaments are thought to define the boundaries of plasma membrane compartments by forming ring-shaped assemblies that provide a barrier to the lateral diffusion of plasma membrane components, including exocyst landmarks (Estey et al., 2010). Septins thereby confine and target vesicle delivery to the site of plasma membrane abscission.

Topologically, plasma membrane abscission resembles both multivesicular body (MVB) formation – a conserved and essential step during endocytic degradation of membrane proteins – and viral budding from a host cell, distinct processes that share a requirement for the endosomal sorting complexes required for transport (ESCRTs) (Hurley and Hanson, 2010). Indeed, certain ESCRT proteins are required for plasma membrane abscission during cytokinesis, at least in cultured mammalian cells (Carlton and Martin-Serrano, 2007; Morita et al., 2007; Carlton et al., 2008). Like septins, members of the ESCRT-III complex form membrane-associated filaments (Hanson et al., 2008), and apparent helices of ESCRT-III filaments at sites of abscission have been detected *in vivo* (Guizetti et al., 2011). In addition, ESCRT-III subunits appear to act more directly in membrane fission, given their ability to induce fission of artificial membranes *in vitro* (Wollert et al., 2009). However, because ESCRT function also regulates vesicular transport, the precise roles of ESCRTs in plasma membrane abscission during cytokinesis remain unclear (Guizetti and Gerlich, 2010).

Septins and ESCRTs were both first identified and characterized in *Saccharomyces cerevisiae*. Septin filaments are essential for budding yeast cytokinesis (McMurray et al., 2011), whereas no defect in cell division has been attributed to the ESCRT mutants, all of which are viable (*Saccharomyces* Genome Database; http://www.yeastgenome.org/). The requirement for septins may reflect important characteristics of yeast budding. The yeast cell wall is dramatically remodeled during cell division, involving deposition of a ‘septum’ of new wall material, especially chitin, which is then resolved to achieve cell separation (Walther and Wendland, 2003; Cabib, 2004). Notably, yeast plasma membrane ingression is driven in part by the cell wall synthesis machinery, and can occur without a contractile ring (Watts et al., 1987; Rodriguez and Paterson, 1990; Bi et al., 1998; Fang et al., 2010), reminiscent of the requirement for different kinds of extracellular matrices in cytokinesis in certain metazoan cell types (Mizuguchi et al., 2003; Izumikawa et al., 2010; Xu and Vogel, 2011). Yeast septins are required for both septation and contractile ring-guided plasma membrane ingression, explaining why they are essential for yeast cell division (Bi, 2001). Furthermore, if septin function is blocked following successful plasma membrane ingression, abscission fails (Dobbelaere and Barral, 2004), indicating an additional requirement for septins in this final step of cytokinesis.

By contrast, yeast ESCRTs were not known to be required in any way for cytokinesis, although vesicular trafficking of certain septation enzymes (e.g., chitin synthase) to and from the plasma membrane at the division site could be affected by ESCRT dysfunction. Interestingly, some archaeal organisms lacking septa and contractile rings assemble ESCRT-III-like polymers at the division site and require them for their binary fission (Samson and Bell, 2009). This phylogenetic curiosity suggests that, if other cytokinetic components are missing or crippled, ESCRTs alone may support plasma membrane abscission. With this

possibility in mind, we reasoned that cells in which cytokinesis is impaired by mutations in known cytokinetic factors might provide a sensitized background where roles for the ESCRT proteins in cell division would be revealed.

Indeed, as described here, mutant phenotypes and genetic interactions strongly suggest that ESCRT components have cytokinetic functions. Our evidence supports a model in which, rather than acting directly in resolution of the plasma membrane during the abscission step of cytokinesis, ESCRT function contributes to proper cytokinesis via vesicular trafficking-mediated modulation of chitin synthase activity at the plasma membrane.

Results

Cytokinesis failure and aberrant DNA content in cells with ESCRT-III defects

Snf7 is the primary component of filaments formed by the ESCRT-III complex, which in yeast also contains the related proteins Vps2, Vps20, and Vps24. Vps20 nucleates Snf7 polymerization on membranes (Teis et al., 2008; Saksena et al., 2009), whereas Vps24 incorporation is thought to both cap the growing filament and recruit Vps2 (Babst et al., 2002; Teis et al., 2008), which activates a catalytic filament disassembly factor, Vps4 (Babst et al., 1998, 2002). Bro1, the yeast ortholog of the human programmed cell death 6 interacting protein (PDCD6IP; Alix) protein critical for ESCRT-III function in retroviral budding, binds Snf7 via a so-called Brol domain equivalent to the same domain in Alix that binds chromatin modifying protein 4 (CHMP4) proteins, the human Snf7 orthologs (Kim et al., 2005; McCullough et al., 2008). Preventing Alix-CHMP4 interaction inhibits cytokinetic abscission in mammalian cells (Carlton et al., 2008). Conversely, driving yeast Bro1-Snf7 association by overexpressing full-length Bro1, or the Bro1 domain alone, enhances the stability of ESCRT-III by inhibiting Vps4-mediated disassembly *in vivo* and *in vitro* (Wemmer et al., 2011).

While examining vesicular morphology in ESCRT mutant cells by thin-section electron microscopy (TEM) (Wemmer et al., 2011), we noticed cells with multiple buds that had not completed cell division (Figure 1A), clear evidence of failed cytokinesis. Although such cells were observed infrequently, they were much rarer in wild-type cultures (data not shown). We also found an unexpected phenotype for Bro1-overexpressing cells that further stimulated our interest. Specifically, cultures of cells overexpressing Brol often achieved higher optical densities (at 600 nm) than other genotypes cultured in the same medium for the same time, yet did not exhibit any difference in doubling time during exponential growth (Megan Wemmer and Greg Odorizzi, unpublished observations). Increased light scattering suggested that excess Brol causes an increase in cell size and/or a failure of cell separation, both potential features of cytokinesis defects.

Insufficient cell division also leads to the accumulation of cells with a DNA content of 2C (or higher) if DNA synthesis occurs but cytokinesis fails. Thus, we measured cellular DNA content by flow cytometry after staining with the fluorescent dye propidium iodide (PI). Indeed, there was a dramatic accumulation of cells with ≥ 2C DNA content in cultures overexpressing Brol (Figure 1B). Moreover, overexpression of the Bro1 domain alone [residues 1–387, here-after Bro1 (1–387)] was sufficient to cause the same phenotype (Figure 1B). Based on these results, we then examined yeast strains deleted for *SNF7, VPS2, VPS4, VPS20, VPS24, BRO1*, or genes encoding components of ESCRT-I (*VPS23*) or -II (*VPS36*), which are required for the early steps in MVB biogenesis (Hurley, 2010). Strikingly, two of the ESCRT-III mutant strains, *snf7Δ vps24Δ*, also showed evidence of aberrant DNA content, as judged by the accumulation of cells delayed during DNA replication (DNA content between 1C and 2C), and an increased proportion of cells with DNA content higher than 2C (Figure 1B). By comparison, the other mutants we examined

did not display pronounced differences from the wild-type (Figure 1C). When others conducted automated analysis of the morphology of the available collection of viable deletion mutants (*Saccharomyces cerevisiae* Morphology Database; http://yeast.gi.k.u-tokyo.ac.jp/), they reported that *snf7Δ* mutants exhibit an abnormally high proportion of medium-budded cells, which, considering that bud emergence coincides with the onset of the S phase, suggests an apparent S phase delay, is consistent with our findings. Moreover, when we analyzed those published micrographs for evidence of cell division defects in *snf7Δ* mutants, we found slightly more multiply-budded cells (two out of 335 cells; 0.6%) and cells with multiple nuclei (two out of 335 cells; 0.6%) than in a control *his3Δ* strain (zero multibudded and one multinucleate out of 370 cells; 0.3%). Taken together with our initial TEM observations and the appearance of an increased >2C population in *snf7* mutant cells, these findings suggested a possible involvement of ESCRT function in yeast cell division.

Genetic interactions between ESeRT-III mutations and *cla4Δ* or *elm 1Δ*

Septin assembly and/or function are perturbed by deletions of certain non-septin genes (for a review, see Longtine and Bi, 2003; McMurray and Thorner, 2009), and these mutants, while viable, display temperature-sensitive phenotypes. For example, although each also functions in distinct processes, the protein kinases Cla4, Elm1, Gin4, Hsll, and Kcc4 contribute to the efficiency and/or temporal dynamics of higher-order septin assembly. Cla4 and Gin4 phosphorylate septins (Mortensen et al., 2002; Versele and Thorner, 2004), whereas Elml phosphorylates Gin4 (Asano et al., 2006) and Hsll (Szkotnicki et al., 2008), and thus indirectly influences septin assembly. Hsll activity at the bud neck regulates cell cycle progression in response to defects in septin assembly (Barral et al., 1999; Shulewitz et al., 1999); consequently, *hsllΔ* mutants are delayed in G2-M. Deletion of the bud neck-associated kinase Kcc4, which physically interacts with septins (Okuzaki and Nojima, 2001), but whose physiological substrates are unknown, displays genetic interactions that place it in a pathway together with Gin4 and Hsll, but separate from Elm1, in the regulation of cytokinesis (Bouquin et al., 2000). The Nap1 protein co-purifies with septins, Gin4, and Kcc4 (Gavin et al., 2002; Mortensen et al., 2002), and *nap1Δ* affects Gin4 activity and bud neck localization (Longtine et al., 2000). *SIZI* encodes an enzyme responsible for small ubiquitin-like modifier (SUMO)-ylation of Cdc3, Cdc11, and Shs1 (Johnson and Gupta, 2001; Takahashi et al., 2001), and the *siz1Δ* allele displays genetic interactions with *shs1Δ* and *nap1Δ* (Collins et al., 2007; Costanzo et al., 2010). Thus, such mutations provide sensitized genetic back-grounds for the analysis of the effects on cytokinesis of mutations in other genes.

For this reason, we combined viable non-septin gene deletions (*cla4Δ, elmlΔ, gin4tl, hsllΔ, kcc4Δ, naplΔ*, or *siz1Δ*) that impede cytokinesis via the effects on septin assembly and/or function (Bouquin et al., 2000; Longtine et al., 2000; Gladfelter et al., 2004) with a *snf7Δ* mutation by mating the corresponding haploid strains, which are all viable. After sporulation of the resulting diploid, meiotic progeny containing both mutant alleles were identified. All of these haploid double mutants were viable at room temperature (RT) on standard rich dextrose-based medium, yeast peptone dextrose (YPD) (data not shown). However, cultivation at higher temperatures revealed a drastic effect of combining *snf7Δ* with *cla4Δ* or *elmlΔ* (Figure 2A), whereas *snf7Δ* alone only mildly impeded colony growth at 37°C and had no detectable effect at 30°C (Figure 2A and data not shown). Specifically, at both 30°C and 37°C, *cla4Δ SNF7*$^{+}$ spore clones formed colonies indistinguishable from those of wild-type cells, but *cla4Δ snf7Δ* colony growth was severely inhibited at 30°C and almost completely blocked at 37°C (Figure 2A). Similarly, colony growth of *snf7Δ elmlΔ* cells was markedly reduced at 37°C (although the effect at 30°C was less pronounced) (Figure 2A).

By contrast, combining *snf7Δ* with *gin4Δ, hsl1Δ, kcc4Δ, nap1Δ*, or *siz1Δ* did not affect colony size (Figure 2A).

Importantly, restoring *CLA4* or *ELM1* on plasmids rescued the growth at 37°C of *cla4Δ snf7Δ* and *elmlΔ snf7Δ* cells, respectively (Figure 2B). Moreover, for *ELM1*, the efficiency of rescue correlated with copy number of the plasmid (Figure 2B). Furthermore, providing otherwise wild-type [but FLAG-tagged; (AspTyrLysAspAspAspAspLys)] Snf7 on a plasmid also rescued growth at 37°C of both *cla4Δ snf7Δ* and *elmlΔ snf7Δ* strains, whereas a plasmid encoding FLAG-tagged Snf7 (L121D), a mutant known to be defective for polymerization *in vitro* and *in vivo* (Saksena et al., 2009), failed to complement the lethality of *cla4Δ snf7Δ* cells at 37°C (Figure 2B). Strikingly, the Snf7 (L12lD) mutant acted in an apparently dominant-negative manner, preventing growth at 37°C of *cla4Δ SNF7*$^{+}$ cells (Figure 2B), possibly by incorporating into and terminating growing ESCRT-III polymers. In addition, consistent with our findings, in a genome-wide synthetic genetic array analysis (Costanzo et al., 2010), *elmlΔ* strains exhibited synthetic colony growth defects at 30°C when combined with a *vps4Δ* mutation *snf7Δ* was not included in that study). Our results demonstrate that otherwise subtle cytokinesis defects caused by deletion of either of two protein kinases known to promote proper septin assembly are exacerbated by loss of ESCRT-III function. Thus, by compromising assembly of higher-order septin structures, we were able to show that ESCRT-III function contributes positively to the process of yeast cell division.

Genetic interactions between ESCRT-III mutations and *cdc10*

We next looked for genetic interactions between mutations in genes encoding ESCRT-III components and in genes encoding septins. The septin genes were first identified via temperature-sensitive point mutations that prevent cytokinesis at the non-permissive temperature (Hartwell, 1971). Subsequent analysis (Sirajuddin et al., 2009) revealed that nearly all temperature-sensitive alleles in *CDC3, CDC10, CDC11* or *CDC12* (Cid et al., 1998; Casamayor and Snyder, 2003; Nagaraj et al., 2008) alter residues predicted to contact the guanine nucleotide that each septin normally binds, and targeted mutations designed to eliminate nucleotide binding in each of these four septins also individually make cells temperature-sensitive for cytokinesis (Versele and Thorner, 2004; Nagaraj et al., 2008; Sirajuddin et al., 2009). The *cdc10-1* allele was isolated in the original cell division cycle screen (Hartwell, 1971) and carries a single base-pair change causing a D182N substitution (Michael A. McMurray and Jeremy Thorner, unpublished results). D182 is situated with-in the so-called G4 motif of the highly conserved guanine nucleotide binding pocket (Sirajuddin et al., 2009), and mutations that abrogate nucleotide binding destabilize septin hetero-oligomers *in vitro* and *in vivo* (Bertin et al., 2008; Nagaraj et al., 2008). In the case of *cdc1O-1*, this instability is manifested as slow colony growth at 30°C and lethality at 37°C (Figure 2C). Considering that Cla4-dependent phosphorylation of Cdc10, like nucleotide binding, promotes higher-order septin assembly *in vivo* (Caviston et al., 2003; Dobbelaere et al., 2003; Kadota et al., 2004; Versele and Thorner, 2004), we expected that *snf7Δ* might exacerbate the phenotype of *cdc10-1* cells, as seen for *cla4Δ snf7Δ* double mutants. However, loss of Snf7 clearly improved the proliferation of *cdc10-1* cells at 30°C (Figure 2C). Consistent with these findings, others have shown that a different ESCRT-III mutation, *vps24Δ*, partially suppresses the colony growth defect at 30°C of cells carrying a different temperature-sensitive allele, *cdc10-4* (Costanzo et al., 2010).

If the improvement in colony growth in *cdc10-1* cells conferred by an ESCRT-III mutation reflects more efficient cytokinesis, then such double mutants should segregate cellular contents more faithfully than *cdc10-1* cells. A characteristic defect of failed cytokinesis in septin mutant cells is the accumulation of multiple nuclei, resulting from mitosis within an undivided cell (Hartwell, 1971). Indeed, DNA staining with 4,6-diamidino-2-phenylindole

(DAPI) revealed that 60% (223/373) of *cdc10-1 SNF7*$^{+}$ cells cultured at 30°C possess multiple nuclei (Figure 2D). By contrast, multinucleate cells were much less frequent in *cdc10-1 snf7Δ* cells at the same temperature (86/382, 23%; one-tailed Fisher's exact test, $p<0.0001$). Thus, when the stability of septin-based structures is compromised, loss of ESCRT-III function improves the ability of cells to carry out their division.

ESCRT-III and septin localization patterns and effects on morphogenesis during normal and defective cell division

Mutants with subtle defects in cytokinesis display an elongated morphology resulting from a delay in the switch from polar to isotropic bud growth. The delay occurs prior to the onset of cytokinesis and is an active response to defects in septin ring assembly (Barral et al., 1999; Shulewitz et al., 1999). Eliminating this morphogenesis checkpoint allows cytokinesis to begin without delay, but often has dire consequences for the completion of cell division (Barral et al., 1999; Bouquin et al., 2000). Thus, elongated cell morphology is a symptom, not a cause, of many cytokinesis defects (in particular, those originating from problems with septin assembly). Hence, monitoring changes in morphology can provide useful information, especially when combined with visualization of septin organization *in vivo* using fluorescently labeled subunits. Therefore, we examined the morphology of cells carrying mutations in various ESCRT factors using transmitted light microscopy. At 30°C, *vps36Δ* (ESCRT-II), *snf7Δ* (ESCRT-III), and *vps4Δ* (ESCRT-III) mutants were indistinguishable in shape from wild-type cells (Figure 3A, C), consistent with the conclusion from our aforementioned TEM analysis that abnormally shaped cells are rare in *snf7Δ* populations and in agreement with the results of a high-throughput study conducted by automated morphometric analysis (*Saccharomyces cerevisiae* Morphology Database; http://yeast.gi.k.u-tokyo.ac.jp/). Moreover, in *snf7Δ* cells, septin structures (marked with Cdc10-mCherry) exhibited the normal distribution of single rings, hourglass-shaped collars, and split rings at the bud neck, indistinguishable from those in wild-type cells (Figure 3B and data not shown).

However, when an ESCRT-III mutation was combined with mutations known to cause modest cytokinesis defects, there were pronounced effects on morphology, especially after a 3-h shift to 37°C, which were not displayed by the single mutants alone. Unlike *snf7Δ* cells, which had a uniformly normal shape (Figure 3C, upper row of images), or *elm1Δ* cells, which grew as clusters of unseparated, elongated cells (Figure 3C, middle row of images), a *snf7Δ elm1Δ* double mutant had a markedly elongated (usually single) bud with multiple obvious constrictions (arrowheads) (Figure 3C, bottom row of images). Considering that *snf7Δ elm1Δ* cells cannot form colonies at this temperature (Figure 2), this morphology presumably represents the terminal phenotype.

By contrast, at 30°C, both *cdc10-1 SNF7*$^{+}$ and *cdc10-1 snf7Δ* cells were only slightly elongated (Figure 3D). In cultures of either genotype, occasional highly elongated and often apparently lysed cells (Figure 3D, arrow) were found at similar frequency (data not shown). However, *cdc10-1 SNF7*$^{+}$ cultures had many mother cells with multiple attached buds (Figure 3D, arrowheads), whereas *cdc10-1* cells lacking Snf7 appeared to complete cytokinesis more frequently, in agreement with our finding that absence of Snf7 improved *cdc10-1* colony growth (Figure 2C). The *cdc10-1* allele that is the sole source of Cdc10 in these cells also harbored a C-terminal green fluorescent protein (GFP) tag, which we used to visualize septin assembly (*GFP* images) and, using this marker, Cdc10 was clearly found at the necks of most buds in the form of collars or split rings, regardless of whether the cells expressed Snf7 (Figure 3D). Thus, at 30°C, the *cdc10-1* allele triggers only a modest morphogenesis checkpoint response, indicating that initial septin collar assembly is largely normal, and suggesting that defects in its stability or organization are manifested only at a

later cell cycle stage. In such cells, absence of Snf7 facilitates execution of events that improve the efficiency of cell division.

If ESCRT-III functions directly in the late steps of cytokinesis, ESCRT-III components should localize to the bud necks of these cells. To address this prediction, we examined Snf7 localization in wild-type cells and in cells in which cytokinesis was perturbed. First, we used a Snf7-0FP fusion expressed from a plasmid in *SNF7*$^{+}$ *CDC10*$^{+}$ or *SNF7*$^{+}$ *cdc10Δ* cells. Cells can tolerate deletion of *CDC10* because the remaining septin proteins are capable of interacting in ways that allow filament assembly, but these mutants are temperature-sensitive and, even at permissive growth temperatures, display noticeable defects, like abnormally wide bud necks (McMurray et al., 2011). As shown in Figure 3E, in cells of either genotype, Snf7-GFP localized to the periphery of the vacuole or as discrete puncta that were randomly distributed in the cytoplasm with relation to the bud neck. The puncta correspond to endosomes as well as 'class E' compartments – abnormal endosomal intracellular structures indicative of impaired ESCRT function – and are a manifestation of the fact that, as is true for other large C-terminal appendages to Snf7, this GFP fusion is partially dysfunctional and inhibits ESCRT-II1 function in a semi-dominant manner (Teis et al., 2008). The lack of any obvious bud neck localization of Snf7-GFP in wild-type cells was also clearly visualized by co-expressing Cdc10-mCherry to mark the neck (Figure 3F). Similarly, Snf7 has been observed only as discrete puncta in previously-published immunofluorescence experiments using fixed wild-type cells and antibodies recognizing endogenous Snf7 (Babst et al., 1998, 2002; Katzmann et al., 2001; Curtiss et al., 2007; Dimaano et al., 2008; Teis et al., 2008). These results argue against a direct role for ESCRT-III as a stable component of the contractile ring. However, the amount of Snf7 at the neck may be below the threshold for detection by these methods or may occur transiently during a short period of the cell cycle that was not well represented in the asynchronous cultures we examined.

To address the latter possibility, and to facilitate the identification of cells in the final stages of cytokinesis, we visualized the contractile ring using a Myol-GFP fusion. Myol appears as a ring at the bud neck that colocalizes with the septin ring just prior to the onset of cytokinesis. The Myol ring then constricts during plasma membrane ingression and ultimately disappears prior to cell separation (Bi et al., 1998; Lippincott and Li, 1998; Vallen et al., 2000). To visualize Snf7 in the same cells, we used a Snf7-mRFP fusion (Huh et al., 2003). Importantly, although each fluorescent reporter is integrated at the corresponding endogenous chromosomal locus, both fluorescently-tagged fusion proteins display evidence of dysfunction due to deleterious influences of their respective tags. Specifically, like Snf7-GFP, Snf7-mRFP also accumulates in class E compartments (Huh et al., 2003). Similarly, Myol-GFP, unlike native Myol expressed in the same manner [from a tetracycline-repressible promoter (Mnaimneh et al., 2004) that replaced the endogenous *MYO1* promoter], was unable to support the growth of *cdc10Δ* cells (M.A.M. and J.T., unpublished observations).

Thus, to provide wild-type ESCRT-III and contractile ring function, a *SNF7-mRFP*-expressing haploid was mated with a *MY01-GFP*-expressing haploid, creating a diploid strain with one wild-type (untagged) copy of each gene. In these diploid cells, Snf7-mRFP frequently colocalized with Myol-GFP at the bud neck (Figure 3G, left column, arrowheads). The fluorescent signal we detected with our RFP filters was not the result of bleed-through from GFP, because other cells within the same field of cells had bright Myol-GFP signal at the neck, but no detectable RFP (Figure 3G, right column). Snf7-mRFP was also found away from the neck, presumably in class E compartments (Figure 3G). Importantly, Snf7-mRFP colocalization with Myol-GFP was only observed prior to contractile ring constriction, when Myol-GFP was present as a relatively large, bright ring

(Figure 3G). Moreover, Snf7-mRFP was never found as a ring at the bud neck in cells with untagged Myol (data not shown), suggesting that the Myol-GFP construct helped 'trap' Snf7-mRFP at the neck, apparently in a semi-dominant fashion. However, Myol depletion (initiated by tetracycline-dependent repression) was not sufficient to drive Snf7-mRFP to the bud neck; after a 5-h or even overnight exposure to tetracycline, only the characteristic punctate Snf7-mRFP pattern was observed in such cells (Supplementary Figure 1, and data not shown). Although Snf7-mRFP accumulated at the site of cytokinesis in some cells when bud necks contained Myol-GFP, we interpret this result with caution, because it could represent a non-physiological situation arising from the use of two functionally compromised fluorescent fusions. Nevertheless, we never observed Snf7-mRFP at the bud neck during the stage of the cell cycle when plasma membrane abscission is thought to occur.

EseRT-I, -II, and -III mutations in *elm1Δ* cells exacerbate cytokinesis defects, elevate chitin synthase II levels, and cause ectopic chitin deposition

Roles for ESCRT complexes in cytokinesis in other cell types are largely restricted to ESCRT-III. However, it was noted that mutations in other ESCRT complexes, including *vps27Δ* (ESCRT-0) and *vps25Δ* (ESCRT-II), inhibit colony growth when combined with an *elm1Δ* mutation (Costanzo et al., 2010). We confirmed the deleterious genetic interaction between *vps27Δ* and *elm1Δ* (Figure 4A) and, in addition, found that *vps23Δ* (ESCRT-I) and *vps36Δ* (ESCRT-II) have a similar negative effect on *elm1Δ* colony growth (Figure 4A). Thus, in cells lacking Elml, there is a greater demand for proper endosomal protein sorting, in general, to achieve efficient cytokinesis. We reasoned that chitin synthase II (Chs2, catalytic subunit encoded by *CHS2*), which drives centripetal deposition of the chitin-rich primary septum behind the ingressing plasma membrane (Cabib, 2004), represented a good candidate for a membrane protein with an important role in cytokinesis that is subject to ESCRT-dependent trafficking. We suspected Chs2 because it is short-lived, undergoes internalization in endosome-like vesicles, and is degraded in the vacuole (Chuang and Schekman, 1996; VerPlank and Li, 2005). Thus, through their role in delivering plasma membrane proteins for degradation in the vacuole, ESCRT components are likely necessary for curtailing Chs2 activity at the neck in a timely manner. Indeed, *vps24Δ* (ESCRT-III) mutants display genetic interactions and alterations in chitin levels consistent with this idea (Lesage et al., 2005). If this model is correct, the steady-state level of Chs2 should be elevated in any ESCRT mutant. In *elm1Δ* cells, where failure of proper septin collar assembly prevents retention of other factors required for efficient cytokinesis, we presume that elevated chitin synthesis resulting from the defect in ESCRT function further disturbs the coordination between cell wall and plasma membrane remodeling that is necessary for successful cell division.

To test this overall idea, we examined the level of endogenous Chs2 in extracts of *elm1Δ, elm1Δ vps23Δ, vps23Δ*, elm1Δ vps27Δ, elm1Δ vps36Δ, and elm1Δ snf7Δ cells by immunoblotting. To optimize detection of Chs2, all of the cultures were first treated with the microtubule-depolymerizing agent nocodazole to arrest cells prior to cytokinesis, and then released from the arrest and allowed to progress synchronously to the onset of cytokinesis. Consistent with our hypothesis, the level of Chs2 [normalized to that of a loading control, phosphoglycerate kinase 1 (Pgk1); data not shown] was markedly increased in *elm1Δ* cells carrying each ESCRT mutant examined, as compared to *elm1Δ* cells alone that possessed a functional ESCRT pathway (Figure 4B). These differences could not be attributed to any difference in the efficiency of the cell cycle arrest, because the level of the mitotic cyclin Clb2 was roughly equivalent in each culture (Figure 4B). The *snf7Δ* mutation resulted in the highest level of Chs2 accumulation (~18-fold elevation), a *vps36Δ* mutation caused a less striking increase (~threefold elevation), and a *vps23Δ* mutation was intermediate (~eightfold

elevation). If excess Chs2 activity is also detrimental to cytokinesis in wild-type cells, the extent of the Chs2 increase caused by different ESCRT mutations may explain why we were able to detect evidence, albeit subtle, for defective cytokinesis in *snf7Δ* cells, but not in *vps23Δ* or *vps36Δ* cells (Figure 1B,C).

Why would *elm1Δ* mutants be especially sensitive to increases in Chs2 activity? In wild-type cells, Chs2 is largely restricted to the bud neck during cytokinesis, in part by the diffusion barrier function of the septin collar at the bud neck. In mutants, like *elm1Δ* (Sreenivasan and Kellogg, 1999; Bouquin et al., 2000) and *cla4Δ* (Schmidt et al., 2003; Versele and Thorner, 2004), in which septin collar assembly is defective, aberrant septin structures form at ectopic locations away from the neck, such as at the tips of elongated buds. At these locations, Chs2 is also found, along with constriction-competent Myol assemblies, that together drive formation of small, abnormal, septum-like structures (Slater et al., 1985; Roh et al., 2002). Hence, as a further test of our prediction that ESCRT mutations increase Chs2 activity at both the bud neck and at ectopic locations in *elm1Δ* cells, we analyzed the deposition of cell wall chitin by staining with Calcofluor White, a fluorescent chitin-binding dye (Pringle, 1991). In cultures grown to saturation at room temperature, the majority of the cells had a near-normal morphology (data not shown); however, dusters of highly elongated cells were readily detectable (Figure 4C). In *elm1Δ* cells, Calcofluor staining (arrowheads) was restricted almost exclusively to the necks of the elongated buds, whereas in *elm1Δ* cells lacking Snf7, Vps23, Vps27 or Vps36, intense staining also was observed at numerous locations along the length of the buds, coinciding with obvious constrictions in the cell wall (Figure 4C). Thus, in the *elmlΔ* cells, lack of a functional ESCRT pathway markedly affected where and how much chitin synthesis occurred, especially at sites away from the bud neck, and is fully consistent with our observation that ESCRT function is needed to maintain the amount of Chs2 at a low level.

Discussion

Taken together, while the results described above indicate that the ESCRT machinery plays no more than a minor role in cytokinesis in wild-type yeast cells, its contribution can be revealed when cytokinesis is hindered by mutations in other, more critical factors. In these cases, ESCRT mutations had either positive or negative effects, depending on the nature of the other defect with which they were combined. Deletion of *SNF7*, encoding the primary component of ESCRT-III filaments, exacerbated division defects in *cla4Δ* and *elm1Δ* cells at 37°C, but alleviated division defects in *cdc10-1* cells at 30°C.

It is difficult to imagine how a direct role for ESCRT-III in yeast plasma membrane abscission during cytokinesis – analogous to what has been proposed in cultured mammalian cells – could account for our observations. One might speculate that, in mutant cells where plasma membrane ingression occurs in a disorganized fashion, such as when the contractile ring fails to properly constrict and ingression is driven just by centripetal deposition of cell wall material, the edges of the ingressing plasma membrane come into close proximity at a number of places, rather than in a single discrete location, leading to unusual topologies that require special activities (e.g., ESCRT-III) to resolve. Indeed, TEM of *myolΔ chs2Δ* cells reveals evidence of these events in the form of so-called ‘lacunae’, pockets of cytosol trapped within the septal material (Schmidt et al., 2002). Although we do not dismiss this possibility, it does not explain why ESCRT-III function in plasma membrane abscission provides a benefit to or *elmlΔ* cells, but an obstacle to *cdc10* cells. Furthermore, the major ESCRT-III component Snf7 could not be detected at the site of cytokinesis at the time plasma membrane abscission is thought to occur, and was only found there significantly earlier in the process.

We favor an alternative model in which ESCRT mutations exert indirect effects on cytokinesis via reduced endocytic turnover of key, membrane-associated factors that act directly in cell division, such as Chs2. As detailed below, we believe that important differences in the underlying septin alterations distinguish cytokinesis-defective mutants helped by loss of ESCRT function from those harmed by the same mutation.

In elongated buds, septins occasionally localize ectopically to the sides and tips, presumably due to abnormally prolonged interactions between septins and Cdc42 effector proteins there (Gladfelter et al., 2005). Consequently, the molecular machinery necessary for cytokinesis (e.g., the contractile ring) and septation (e.g., Chs2) is also found at these locations, resulting in ectopic plasma membrane invaginations and septum-like cell wall deposits (Roh et al., 2002; Schmidt et al., 2002). These multiple sites of attempted cell division set up a competitive situation that, if some limiting component is in short supply, prevents anyone location from assembling the apparatus needed for the completion of cytokinesis. Temperature-sensitive septin mutants are prone to frequent ectopic assembly of contractile ring and septation components (Slater et al., 1985; Roh et al., 2002; Schmidt et al., 2002). Overexpression of a truncated version of Myo1 lacking its motor domain that is nonetheless sufficient to guide furrow ingression and cell wall remodeling during cytokinesis is able to partially suppress the growth defect of temperature-sensitive septin mutants (Fang et al., 2010). Thus, one factor apparently limiting for cytokinesis when septins are defective is a contractile ring component.

Given that the septation apparatus can also drive furrow ingression (Bi et al., 1998; Fang et al., 2010), Chs2 activity represents another good candidate for a component limiting for cytokinesis in certain septin mutants. Thus, mutations that block endocytic turnover of Chs2 could elevate chitin synthase activity at the neck and improve the efficiency of cytokinesis in these cells. Our findings provide strong support for this idea: ESCRT mutations increase Chs2 levels and partially suppress the slow colony growth and accumulation of multinucleate cells in a septin mutant (*cdc10-1*). Furthermore, an independent allele of *cdc10-4* is similarly suppressed by a *vps24Δ* (ESCRT-III) mutation (Costanzo et al., 2010). Finally, *vps24Δ* cells are hypersensitive to exogenous Calcofluor White (Lesage et al., 2005) or Congo Red in the growth medium (Weiss et al., 2008), indicators of elevated chitin levels (Ram and Klis, 2006).

However, if supplies of required components are just sufficient for cytokinesis at the bud neck, then abortive attempts at sites elsewhere would detrimentally impact successful cell division at the correct location. In *elm1Δ* cells, ESCRT mutations increased Chs2 levels (Figure 4) and caused aberrant constrictions in growing buds (Figures 3 and 4) accompanied by intensified chitin deposits at those sites (Figure 4), which presumably decreased the frequency of successful cleavage at bud necks within a growing colony. In our model, any mutation that prevents Chs2 degradation could similarly elevate Chs2 activity, causing the observed colony growth and cell morphology defects when combined with an *elm1Δ* (or *cla4Δ*) mutation. Indeed, other ESCRT mutants defective in endocytic turnover of plasma membrane proteins, such as *vps27Δ* (ESCRT-0), *vps23Δ* (ESCRT-I), *vps25Δ* (ESCRT-II), or *vps36Δ* (ESCRT-II), also inhibit *elm1Δ* colony growth (Figure 4) (see also Costanzo et al., 2010).

We suspect that the negative effects of *snf7Δ* were manifested in *cla4Δ* or *elm1Δ* cells because the buds in these mutants are generally much more elongated (and inappropriate bud-tip localization of septins is much more pronounced) than *gin4* (Longtine et al., 1998, 2000; Barral et al., 1999), *hsl1* (Barral et al., 1999; Longtine et al., 2000; Thomas et al., 2003), *kcc4Δ* (Barral et al., 1999; Okuzaki and Nojima, 2001), *nap1Δ* (Longtine et al., 2000) or *siz1Δ* cells (Johnson and Gupta, 2001) mutants. Indeed, the primary cytokinesis

defect in cells lacking Cla4 or Elml appears to be a failure to assemble a well-organized septin collar at the bud neck and a corresponding failure to prevent deposition of septin structures at locations away from the bud neck. The actions of Cla4 and Elml contribute to proper septin assembly prior to bud emergence (Blacketer et al., 1995; Kadota et al., 2004; Versele and Thorner, 2004). Cla4 is dispensable for the later steps, because engineered Cla4 degradation following proper septin collar assembly has no effect on cytokinesis (Kadota et al., 2004). Similarly, although Elml clearly has post-G1 functions, these are manifested in *elm1* mutants as delays in entry into (Sreenivasan et al., 2003) and/or exit from (Bouquin et al., 2000) mitosis, whereas bud neck defects in plasma membrane ingression/abscission *per se* have not been observed.

Among all the cytokinesis mutants we tested for synthetic effects with *snf7Δ, cdc10-1* was unique in that increased Chs2 improved the execution of cell division (Figure 3D). What is special about *cdc10-1?* Despite near-normal bud morphology and septin localization at the bud neck (and not elsewhere) in these cells at temperatures permissive for colony growth, cytokinesis frequently fails, yielding cells with multiple (and, sometimes, chains of) buds. Thus, the defect caused by *cdc1 0-1* is presumably not in initiating and fonning a septin collar at the bud neck, but rather in maintaining its structure in a stable and fully functional form at that location. The septins rings that flank the bud neck when the septin collar splits are known to act as a diffusion barrier for Chs2 (Dobbelaere and Barral, 2004). Thus, although the neck is correctly defined as the sole site of exocytic delivery in *cdc10-1* cells, we presume that the resulting split rings fail to maintain their full integrity even at 30°C, preventing proper retention of Chs2 and other factors required for cytokinesis and septation. Given the importance of bound nucleotide in cementing septin-septin interactions (Versele and Thorner, 2004; Nagaraj et al., 2008; Sirajuddin et al., 2009), a defective nucleotide-binding subunit, like Cdc10-1, is likely to impart significant fragility to septin-based structures. We presume, therefore, that the general increase in Chs2 level at the plasma membrane when ESCRT function is crippled by a *snf7Δ* mutation partially compensates for the inability of the weakened split rings in *cdc10-1* cells to retain a sufficient level of Chs2 activity, thereby improving the chance of successful septation. Consistent with this idea, ESCRT mutants (such as *snf7Δ* cells) display increased recycling of internalized plasma membrane proteins (Teis et al., 2008).

Previous studies have demonstrated essential roles for membrane trafficking via the secretory, endocytic, and recycling pathways during cytokinesis. Notably, endocytic membrane internalization occurs at the site of plasma membrane abscission in cultured mammalian cells, termed the midbody, and is required for cytokinesis (Schweitzer et al., 2005). Recycling from endosomal vesicles may play an important role in providing the membrane material necessary to complete animal cell cytokinesis (Finger and White, 2002), and indeed recycling endosomes are found in close proximity to the midbody during a brief period late in mitosis, prior to contractile ring constriction (Schweitzer et al., 2005). Although highly speculative, it is possible that the Snt7-mRFP we observed closely situated near the contractile ring in yeast cells expressing Myo1-GFP represents a related compartment whose existence is too transient to visualize in wild-type cells, and was only detectable in the *SNF7-mRFPI+MY01-GFPI/+* genetic background because the fluorescent tags slightly compromised the function of each fusion protein in a semi-dominant manner, extending the period between contractile ring maturation and constriction, as well as the lifetime of ESCRT assemblies at these internal membranes. In this regard, it is interesting to note that human CHMP4B interacts with the FYVE-CENT/TC19 protein complex found on phosphatidylinositol 3-phosphate (PI3P)-containing membrane compartments at the midbody (Segona et al., 2010). In addition, Bro1, a regulator of yeast ESCRT-III disassembly and membrane scission activity (Wemmer et al., 2011), and Hof1, an important regulator of yeast cytokinesis associated with the contractile ring prior to its constriction

(Vallen et al., 2000; Blondel et al., 2005; Nishihama et al., 2009), reportedly interact, at least as judged by the yeast two-hybrid method (Tonikian et al., 2009). This association is reminiscent of the direct interactions of Alix, the mammalian Bro1 ortholog, with various cytokinetic factors, like IQ motif containing GTPase activating protein 1 (IQGAPI) (Morita et al., 2007).

Materials and methods

Yeast strains, plasmids, and cultivation media

Cultivation of yeast strains (Supplementary Table 1) was carried out according to the protocol used by Sherman et al. (1986) in standard dextrose-based rich (YPD) or synthetic complete (SC) media lacking appropriate nutrients to maintain non-essential plasmids (Supplementary Table 2). Sporulation medium was 0.3% potassium acetate and O.02% raffinose. Geneticin® (G418 sulfate; Invitrogen Corporation, Carslbad, CA, USA), hygromycin (Invitrogen Corporation), and/or tetracycline hydrochloride (Sigma-Aldrich, St. Louis, MO, USA) was added to YPD to 300 μg/ml, 150 μg/ml, or 50 μg/ml final concentration, respectively.

Electron microscopy

Yeast cells were high-pressure frozen and freeze-substituted as previously described in (Nickerson et al., 2006; Richter et al., 2007) and embedded at −60°C in Lowicryl HM20 (Polysciences, Inc., Warrington, PA, USA). Plastic blocks were trimmed and cut into 80-nm sections with a Leica microtome (Leica Microsystems, Wetzlar, Germany) and placed on rhodium-plated copper slot grids prior to imaging with a Philips CM10 transmission electron microscope (EM) (FEI™, Hillsboro, Oregon, USA).

Light microscopy

Calcofluor White (Fluorescent brightener 28, Sigma-Aldrich) was used to visualize cell wall chitin as described previously (Pringle, 1991). For visualization of nuclei, cells were fixed with 70% ethanol for 5 min, washed twice with water, and resuspended in 50 ng/ml DAPI (Sigma-Aldrich). As indicated in the Figure legends, micrographs were captured using one of two microscopes. For single focal plane images, a BH-2 microscope (Olympus America, San Jose, CA, USA) equipped with a 60× objective, with a tetramethyl rhodamine iso-thiocyanate (TRITC) filter set (Chroma Technology Corporation, Bellows Falls, VT, USA) to view mRFP, an eGFP filter set (Chroma Technology Corporation) to view GFP, and a UG-1 excitation filter (Chroma Technology Corporation) with no emission filter, to view Calcofluor White and DAPI fluorescence, and digitally captured using a charge-coupled device (CCD) camera (Optronics®, Goleta, CA, USA). To capture images of a given field of cells at various points in the *z* direction, we used a Delta Vision RT microscopy system (Applied Precision, Inc., Issaquah, WA, USA) equipped with an IX71 Olympus microscope, a PlanApo 100× objective (1.35 NA, Olympus), DAPI, fluorescein isothiocyanate (FITC), and rhodamine filters, and a Cool Snap HQ digital camera (Photometrics, Tuscon, AZ, USA). Images were deconvolved using SoftWoRx 3.5.0 software (Applied Precision).

Flow cytometry

Cells were prepared essentially as described by Haase and Lew (1997). Cultures were grown to mid-exponential phase and approximately 1×10^7 cells were washed and fixed in 70% ethanol for 1 h at RT or overnight at 4°C. After fixation, cells were resuspended in 0.5 ml RNase A solution (2 mg/ml in 50 μM Tris-HCI pH 7.5) and incubated for 4 h at 37°C on a platform shaker. Following RNase A treatment, cells were resuspended in 1× propidium iodide (PI) solution (100 μM PI, 180 μM NaCl, 100 mM Tris-HCI pH 7.5), covered in foil and

incubated overnight on a nutator. Cells were either analyzed immediately or stored in the dark at 4°C for subsequent analysis. Cells were diluted approximately 1:5 in 0.1×PI solution for analysis on a CYAN flow cytometer (Beckman Coulter, Inc., Brea, CA, USA) using the PE-Texas Red channel (FL3) and a parameter for cell cycle analysis of fixed cells. The side-scatter voltage was 450–470 V; gain 1.5; forward-scatter gain, 14. During analysis, the event rate was maintained at 200–300 per second.

Cell cycle synchrony, preparation of protein extracts and immunoblotting

Five-milliliter YPD cultures in late exponential phase at 30°C were first permeabilized by the addition of 50 μ1 dimethyl sulfoxide (DMSO) and incubation at 30°C for 30 min, then arrested in mitosis by the addition of 50 μ1 1.5 mg/ml nocodazole (dissolved in DMSO; Sigma-Aldrich), followed by incubation at 30°C for 3 h. To enrich for cells undergoing cytokinesis, the arrested cultures were washed three times with 10 ml YPD, resuspended in 5 ml YPD, and incubated for 1 h at 30°C. At this point, the *CHS2-GFP* strain YEF3923 was used to confirm that Chs2 was located at the bud neck in approximately 70% of cells (data not shown). Total cellular protein was extracted by alkaline lysis followed by precipitation with trichloroacetic acid and extraction into 50 μl of sodium dodecyl sulfate polyacrylamide gel electrophoresis (SDS-PAGE) sample buffer (Riezman et al., 1983). After boiling for 5 min, 20 μl portions of these samples were resolved by SDS/PAGE (10% acrylamide) and transferred to nitrocellulose. The membrane was cut horizontally at the location of a pre-stained 84-kDa molecular weight standard (bovine serum albumin), and the top portion was blocked with 5% skimmed milk in tris-buffered saline (TBS) for 15 min and then incubated overnight with anti-Chs2 antibodies (a gift of Randy Schekman, University of California, Berkeley, CA, USA) diluted 1:10 000 in 2.5% milk in TBS. The bottom portion was blocked with Odyssey Block (LI-COR Biosciences, Lincoln, NE, USA) for 1 h before incubation with affinity-purified rabbit anti-Clb2 antibody (diluted 1:4 000, a gift of Doug Kellogg, University of California, Santa Cruz, CA, USA) and rabbit polyclonal anti-Pgkl antiserum (diluted 1:10 000; Baum et al., 1978). After washing, blots were incubated with appropriate secondary antibodies conjugated to infrared fluorophores, and visualized using an Odyssey infrared imaging system (LI-COR).

Supplementary Material

Refer to Web version on PubMed Central for supplementary material.

Acknowledgments

We thank Doug Kellogg (University of California, Santa Cruz, CA, USA) for the anti-Clb2 antibody, Randy Schekman (University of California, Berkeley, CA, USA) for the anti-Chs2 antibody and members of his lab for assistance with its use, and Erfei Bi (University of Pennsylvania Medical School, Philadelphia, PA, USA) for sharing unpublished reagents and helpful advice. This work was supported by funds from the National Institutes of Health of the United States of America (GM-07135 to M.W, GM-065505 to G.O., GM-86603 to M.A.M., and GM-21841 to J.T.) and by funds from the Weill Institute for Cell and Molecular Biology (to S.D.E.).

References

Asano S, Park JE, Yu LR, Zhou M, Sakchaisri K, Park CJ, Kang YH, Thorner J, Veenstra TD, Lee KS. Direct phosphorylation and activation of a Nim1-related kinase Gin4 by Elm1 in budding yeast. J. Biol. Chem. 2006; 281:27090–27098. [PubMed: 16861226]

Babst M, Wendland B, Estepa EJ, Emr SD. The Vps4p AAA ATPase regulates membrane association of a Vps protein complex required for normal endosome function. EMBO J. 1998; 17:2982–2993. [PubMed: 9606181]

Babst M, Katzmann DJ, Estepa-Sabal EJ, Meerloo T, Emr SD. Escrt-III: an endosome-associated heterooligomeric protein complex required for mvb sorting. Dev. Cell. 2002; 3:271–282. [PubMed: 12194857]

Baum P, Thorner J, Honig L. Identification of tubulin from the yeast *Saccharomyces cerevisiae*. Proc. Natl. Acad. Sci. USA. 1978; 75:4962–4966. [PubMed: 368805]

Barral Y, Parra M, Bidlingmaier S, Snyder M. Niml-related kinases coordinate cell cycle progression with the organization of the peripheral cytoskeleton in yeast. Genes Dev. 1999; 13:176–187. [PubMed: 9925642]

Bertin A, McMurray MA, Grob P, Park SS, Garcia G 3rd, Patanwala I, Ng HL, Alber T, Thorner J, Nogales E. *Saccharomyces cerevisiae* septins: supramolecular organization of heterooligomers and the mechanism of filament assembly. Proc. Natl. Acad. Sci. USA. 2008; 105:8274–8279. [PubMed: 18550837]

Bi E. Cytokinesis in budding yeast: the relationship between actomyosin ring function and septum formation. Cell Struct. Funct. 2001; 26:529–537. [PubMed: 11942606]

Bi E, Maddox P, Lew DJ, Salmon ED, McMillan JN, Yeh E, Pringle JR. Involvement of an actomyosin contractile ring in *Saccharomyces cerevisiae* cytokinesis. J. Cell Biol. 1998; 142:1301–1312. [PubMed: 9732290]

Blacketer MJ, Madaule P, Myers AM. Mutational analysis of morphologic differentiation in *Saccharomyces cerevisiae*. Genetics. 1995; 140:1259–1275. [PubMed: 7498768]

Blondel M, Bach S, Bamps S, Dobbelaere J, Wiget P, Longaretti C, Barral Y, Meijer L, Peter M. Degradation of Hofl by SCF (Grr1) is important for actomyosin contraction during cytokinesis in yeast. EMBO J. 2005; 24:1440–1452. [PubMed: 15775961]

Bouquin N, Barral Y, Courbeyrette R, Blondel M, Snyder M, Mann C. Regulation of cytokinesis by the Elml protein kinase in *Saccharomyces cerevisiae*. J. Cell Sci. 2000; 113:1435–1445. [PubMed: 10725226]

Cabib E. The septation apparatus, a chitin-requiring machine in budding yeast. Arch. Biochem. Biophys. 2004; 426:201–207. [PubMed: 15158670]

Carlton JG, Martin-Serrano J. Parallels between cytokinesis and retroviral budding: a role for the ESCRT machinery. Science. 2007; 316:1908–1912. [PubMed: 17556548]

Carlton JG, Agromayor M, Martin-Serrano J. Differential requirements for Alix and ESCRT-III in cytokinesis and HIV-l release. Proc. Natl. Acad. Sci. USA. 2008; 105:10541–10546. [PubMed: 18641129]

Casamayor A, Snyder M. Molecular dissection of a yeast septin: distinct domains are required for septin interaction, localization, and function. Mol. Cell. Biol. 2003; 23:2762–2777. [PubMed: 12665577]

Caviston JP, Longtine M, Pringle JR, Bi E. The role of Cdc42p GTPase-activating proteins in assembly of the septin ring in yeast. Mol. Biol. Cell. 2003; 14:4051–4066. [PubMed: 14517318]

Chuang JS, Schekman RW. Differential trafficking and timed localization of two chitin synthase proteins, Chs2p and Chs3p. J. Cell Biol. 1996; 135:597–610. [PubMed: 8909536]

Cid VJ, Adamikova L, Cenamor R, Molina M, Sánchez M, Nombela C. Cell integrity and morphogenesis in a budding yeast septin mutant. Microbiology. 1998; 144:3463–3474. [PubMed: 9884239]

Collins SR, Miller KM, Maas NL, Roguev A, Fillingham J, Chu CS, Schuldiner M, Gebbia M, Recht J, Shales M, et al. Functional dissection of protein complexes involved in yeast chromosome biology using a genetic interaction map. Nature. 2007; 446:806–810. [PubMed: 17314980]

Costanzo M, Baryshnikova A, Bellay J, Kim Y, Spear ED, Sevier CS, Ding H, Koh JL, Toufighi K, Mostafavi S, et al. The genetic landscape of a cell. Science. 2010; 327:425–431. [PubMed: 20093466]

Curtiss M, Jones C, Babst M. Efficient cargo sorting by ESCRT-I and the subsequent release of ESCRT-I from multivesicular bodies requires the subunit Mvbl2. Mol. Biol. Cell. 2007; 18:636–645. [PubMed: 17135292]

Dimaano C, Jones CB, Hanono A, Curtiss M, Babst M. Istl regulates Vps4 localization and assembly. Mol. Biol. Cell. 2008; 19:465–474. [PubMed: 18032582]

Dobbelaere J, Barral Y. Spatial coordination of cytokinetic events by compartruentalization of the cell cortex. Science. 2004; 305:393–396. [PubMed: 15256669]

Dobbelaere J, Gentry MS, Hallberg RL, Barral Y. Phosphorylation-dependent regulation of septin dynamics during the cell cycle. Dev. Cell. 2003; 4:345–357. [PubMed: 12636916]

Estey MP, Di Ciano-Oliveira C, Froese CD, Bejide MT, Trimble WS. Distinct roles of septins in cytokinesis: SEPT9 mediates midbody abscission. J. Cell Biol. 2010; 191:741–749. [PubMed: 21059847]

Fang X, Luo J, Nishihama R, Wloka C, Dravis C, Travaglia M, Iwase M, Vallen EA, Bi E. Biphasic targeting and cleavage furrow ingression directed by the tail of a myosin II. J. Cell Biol. 2010; 191:1333–1350. [PubMed: 21173112]

Finger EP, White JG. Fusion and fission: membrane trafficking in animal cytokinesis. Cell. 2002; 108:727–730. [PubMed: 11955425]

Gavin AC, Bösche M, Krause R, Grandi P, Marzioch M, Bauer A, Schultz J, Rick JM, Michon AM, Cruciat CM, et al. Functional organization of the yeast proteome by systematic analysis of protein complexes. Nature. 2002; 415:141–147. [PubMed: 11805826]

Gladfelter AS, Zyla TR, Lew DJ. Genetic interactions among regulators of septin organization. Eukaryot. Cell. 2004; 3:847–854. [PubMed: 15302817]

Gladfelter AS, Kozubowski L, Zyla TR, Lew DJ. Interplay between septin organization, cell cycle and cell shape in yeast. J. Cell Sci. 2005; 118:1617–1628. [PubMed: 15784684]

Guizetti J, Gerlich DW. Cytokinetic abscission in animal cells. Semin. Cell. Dev. Biol. 2010; 21:909–916. [PubMed: 20708087]

Guizetti J, Schermelleh L, Mantler J, Maar S, Poser I, Leonhardt H, Müller-Reichert T, Gerlich DW. Cortical constriction during abscission involves helices of ESCRT-III-dependent filaments. Science. 2011; 331:1616–1620. [PubMed: 21310966]

Hanson PI, Roth R, Lin Y, Heuser JE. Plasma membrane deformation by circular arrays of ESCRT-III protein filaments. J. Cell Biol. 2008; 180:389–402. [PubMed: 18209100]

Haase SB, Lew DJ. Flow cytometric analysis of DNA content in budding yeast. Methods Enzymol. 1997; 283:322–332. [PubMed: 9251030]

Hartwell LH. Genetic control of the cell division cycle in yeast. IV. Genes controlling bud emergence and cytokinesis. Exp. Cell Res. 1971; 69:265–276. [PubMed: 4950437]

He B, Guo W. The exocyst complex in polarized exocytosis. Curr. Opin. Cell Biol. 2009; 21:537–542. [PubMed: 19473826]

Huh WK, Falvo JV, Gerke LC, Carroll AS, Howson RW, Weissman JS, O'Shea EK. Global analysis of protein localization in budding yeast. Nature. 2003; 425:686–691. [PubMed: 14562095]

Hurley JH. The ESCRT complexes. Crit. Rev. Biochem. Mol. Biol. 2010; 45:463–487. [PubMed: 20653365]

Hurley JH, Hanson PI. Membrane budding and scission by the ESCRT machinery: it's all in the neck. Nat. Rev. Mol. Cell Biol. 2010; 11:556–566. [PubMed: 20588296]

Izumikawa T, Kanagawa N, Watamoto Y, Okada M, Saeki M, Sakano M, Sugahara K, Sugihara K, Asano M, Kitagawa H. Impairment of embryonic cell division and glycosaminoglycan biosynthesis in glucuronyltransferase-I-deficient mice. J. Biol. Chem. 2010; 285:12190–12196. [PubMed: 20164174]

Johnson ES, Gupta AA. An E3-like factor that promotes SUMO conjugation to the yeast septins. Cell. 2001; 106:735–744. [PubMed: 11572779]

Kadota J, Yamamoto T, Yoshiuchi S, Bi E, Tanaka K. Septin ring assembly requires concerted action of polarisome components, a PAK kinase Cla4p, and the actin cytoskeleton in *Saccharomyces cerevisiae*. Mol. Biol. Cell. 2004; 15:5329–5345. [PubMed: 15371547]

Katzmann DJ, Babst M, Emr SD. Ubiquitin-dependent sorting into the multi vesicular body pathway requires the function of a conserved endosomal protein sorting complex, ESCRT-1. Cell. 2001; 106:145–155. [PubMed: 11511343]

Kim J, Sitaraman S, Hierro A, Beach BM, Odorizzi G, Hurley JH. Structural basis for endosomal targeting by the Brol domain. Dev. Cell. 2005; 8:937–947. [PubMed: 15935782]

Kinoshita M, Noda M. Roles of septins in the mammalian cytokinesis machinery. Cell Struct. Funct. 2001; 26:667–670. [PubMed: 11942624]

Lesage G, Shapiro J, Specht CA, Sdicu AM, Ménard P, Hussein S, Tong AH, Boone C, Bussey H. An interactional network of genes involved in chitin synthesis in *Saccharomyces cerevisiae*. BMC Genet. 2005; 6:8. [PubMed: 15715908]

Lippincott J, Li R. Sequential assembly of myosin II, an IQGAP-like protein, and filamentous actin to a ring structure involved in budding yeast cytokinesis. J. Cell Biol. 1998; 140:355–366. [PubMed: 9442111]

Longtine MS, Bi E. Regulation of septin organization and function in yeast. Trends Cell Biol. 2003; 13:403–409. [PubMed: 12888292]

Longtine MS, Fares H, Pringle JR. Role of the yeast Gin4p protein kinase in septin assembly and the relationship between septin assembly and septin function. J. Cell Biol. 1998; 143:719–736. [PubMed: 9813093]

Longtine MS, Theesfeld CL, McMillan JN, Weaver E, Pringle JR, Lew DJ. Septin-dependent assembly of a cell cycle-regulatory module in *Saccharomyces cerevisiae*. Mol. Cell Biol. 2000; 20:4049–4061. [PubMed: 10805747]

McCullough J, Fisher RD, Whitby EG, Sundquist WI, Hill CP. ALIX-CHMP4 interactions in the human ESCRT pathway. Proc. Natl. Acad. Sci. USA. 2008; 105:7687–7691. [PubMed: 18511562]

McMurray MA, Thorner J. Septins: molecular partitioning and the generation of cellular asymmetry. Cell Div. 2009; 4:18. [PubMed: 19709431]

McMurray MA, Bertin A, Garcia G 3rd, Lam L, Nogales E, Thorner J. Septin filament formation is essential in budding yeast. Dev. Cell. 2011; 20:540–549. [PubMed: 21497764]

Mizuguchi S, Uyama T, Kitagawa H, Nomura KH, Dejima K, Gengyo-Ando K, Mitani S, Sugahara K, Nomura K. Chondroitin proteoglycans are involved in cell division of *Caenorhabditis elegans*. Nature. 2003; 423:443–448. [PubMed: 12761550]

Mnaimneh S, Davierwala AP, Haynes J, Moffat J, Peng WT, Zhang W, Yang X, Pootoolal J, Chua G, Lopez A, et al. Exploration of essential gene functions via titratable promoter alleles. Cell. 2004; 118:31–44. [PubMed: 15242642]

Morita E, Sandrin V, Chung HY, Morham SG, Gygi SP, Rodesch CK, Sundquist WI. Human ESCRT and ALIX proteins interact with proteins of the midbody and function in cytokinesis. EMBO J. 2007; 26:4215–4227. [PubMed: 17853893]

Mortensen EM, McDonald H, Yates J 3rd, Kellogg DR. Cell cycle-dependent assembly of a Gin4-septin complex. Mol. Biol. Cell. 2002; 13:2091–2105. [PubMed: 12058072]

Nagaraj S, Rajendran A, Jackson CE, Longtine MS. Role of nucleotide binding in septin-septin interactions and septin localization in *Saccharomyces cerevisiae*. Mol. Cell. Biol. 2008; 28:5120–5137. [PubMed: 18541672]

Nickerson DP, West M, Odorizzi G. Did2 coordinates Vps4-mediated dissociation of ESCRT-III from endosomes. J. Cell Biol. 2006; 175:715–720. [PubMed: 17130288]

Nishihama R, Schreiter JH, Onishi M, Vallen EA, Hanna J, Moravcevic K, Lippincott ME, Han H, Lemmon MA, Pringle JR, Bi E. Role of Inn 1 and its interactions with Hofl and Cyk3 in promoting cleavage furrow and septum formation in *S. cerevisiae*. J. Cell Biol. 2009; 185:995–1012. [PubMed: 19528296]

Odorizzi G, Katzmann DJ, Babst M, Audhya A, Emr SD. Brol is an endosome-associated protein that functions in the MVB pathway in *Saccharomyces cerevisiae*. J. Cell Sci. 2003; 116:1893–1903. [PubMed: 12668726]

Okuzaki D, Nojima H. Kcc4 associates with septin proteins of *Saccharomyces cerevisiae*. FEBS Lett. 2001; 489:197–201. [PubMed: 11165249]

Pringle JR. Staining of bud scars and other cell wall chitin with calcofluor. Methods Enzymol. 1991; 194:732–735. [PubMed: 2005820]

Ram AE, Klis EM. Identification of fungal cell wall mutants using susceptibility assays based on Calcofluor white and Congo red. Nat. Protoc. 2006; 1:2253–2256. [PubMed: 17406464]

Richter C, West M, Odorizzi G. Dual mechanisms specify Doa4-mediated deubiquitination at multi vesicular bodies. EMBO J. 2007; 26:2454–2464. [PubMed: 17446860]

Riezman H, Hase T, van Loon AP, Grivell LA, Suda K, Schatz G. Import of proteins into mitochondria: a 70 kilodalton outer membrane protein with a large carboxy-terminal deletion is still transported to the outer membrane. EMBO J. 1983; 2:2161–2168. [PubMed: 6321150]

Rodriguez JR, Paterson BM. Yeast myosin heavy chain mutant: maintenance of the cell type specific budding pattern and the normal deposition of chitin and cell wall components requires an intact myosin heavy chain gene. Cell Motil. Cytoskeleton. 1990; 17:301–308. [PubMed: 2076546]

Roh DH, Bowers B, Schmidt M, Cabib E. The septation apparatus, an autonomous system in budding yeast. Mol. Biol. Cell. 2002; 13:2747–2759. [PubMed: 12181343]

Sagona AP, Nezis IP, Pedersen NM, Liestøl K, Poulton J, Rusten TE, Skotheim RI, Raiborg C, Stenmark H. PtdIns(3)P controls cytokinesis through KIFI3A-mediated recruitment of FYVE-CENT to the midbody. Nat. Cell Biol. 2010; 12:362–371. [PubMed: 20208530]

Saksena S, Wahlman J, Teis D, Johnson AE, Emr SD. Functional reconstitution of ESCRT-III assembly and disassembly. Cell. 2009; 136:97–109. [PubMed: 19135892]

Samson RY, Bell SD. Ancient ESCRTs and the evolution of binary fission. Trends Microbiol. 2009; 17:507–513. [PubMed: 19783442]

Schmidt M, Bowers B, Varma A, Roh DH, Cabib E. In budding yeast, contraction of the actomyosin ring and formation of the primary septum at cytokinesis depend on each other. J. Cell Sci. 2002; 115:293–302. [PubMed: 11839781]

Schmidt M, Varma A, Drgon T, Bowers B, Cabib E. Septins, under Cla4p regulation, and the chitin ring are required for neck integrity in budding yeast. Mol. Biol. Cell. 2003; 14:2128–2141. [PubMed: 12802080]

Schweitzer JK, Burke EB, Goodson HY, D'Souza-Schorey C. Endocytosis resumes during late mitosis and is required for cytokinesis. J. Biol. Chem. 2005; 280:41628–41635. [PubMed: 16207714]

Sherman, E.; Fink, GR.; Hicks, JB. Laboratory course manual for methods in yeast genetics. Cold Spring Harbor Laboratory Press; Cold Spring Harbor, NY: 1986.

Shulewitz MJ, Inouye CJ, Thorner J. Hs17 localizes to a septin ring and serves as an adapter in a regulatory pathway that relieves tyrosine phosphorylation of Cdc28 protein kinase in *Saccharomyces cerevisiae*. Mol. Cell. Biol. 1999; 19:7123–7137. [PubMed: 10490648]

Sirajuddin M, Farkasovsky M, Zent E, Wittinghofer A. GTP-induced conformational changes in septins and implications for function. Proc. Natl. Acad. Sci. USA. 2009; 106:16592–16597. [PubMed: 19805342]

Slater ML, Bowers B, Cabib B. Formation of septum-like structures at locations remote from the budding sites in cytokinesis-defective mutants of *Saccharomyces cerevisiae*. J. Bacteriol. 1985; 162:763–767. [PubMed: 3886632]

Sreenivasan A, Kellogg D. The elm1 kinase functions in a mitotic signaling network in budding yeast. Mol. Cell. Biol. 1999; 19:7983–7994. [PubMed: 10567524]

Sreenivasan A, Bishop AC, Shokat KM, Kellogg DR. Specific inhibition of Elm1 kinase activity reveals functions required for early G1 events. Mol. Cell. Biol. 2003; 23:6327–6337. [PubMed: 12917352]

Szkotnicki L, Crutchley JM, Zyla TR, Bardes ES, Lew DJ. The checkpoint kinase Hsl1p is activated by Elm1p-dependent phosphorylation. Mol. Biol. Cell. 2008; 19:4675–4686. [PubMed: 18768748]

Takahashi Y, Toh-e A, Kikuchi Y. A novel factor required for the SUMOl/Smt3 conjugation of yeast septins. Gene. 2001; 275:223–231. [PubMed: 11587849]

Teis D, Saksena S, Emr SD. Ordered assembly of the ESCRT-III complex on endosomes is required to sequester cargo during MVB formation. Dev. Cell. 2008; 15:578–589. [PubMed: 18854142]

Thomas CL, Blacketer MJ, Edgington NP, Myers AM. Assembly interdependence among the *S. cerevisiae* bud neck ring proteins Elmlp, Hsllp and Cdc12p. Yeast. 2003; 20:813–826. [PubMed: 12845607]

Tonikian R, Xin X, Toret CP, Gfeller D, Landgraf C, Panni S, Paoluzi S, Castagnoli L, Currell B, Seshagiri S, et al. Bayesian modeling of the yeast SH3 domain interactome predicts spatiotemporal dynamics of endocytosis proteins. PLoS Biol. 2009; 7:e1000218. [PubMed: 19841731]

Vallen EA, Caviston J, Bi E. Roles of Hoflp, Bnilp, Bmlp, and myolp in cytokinesis in *Saccharomyces cerevisiae*. Mol. Biol. Cell. 2000; 11:593–611. [PubMed: 10679017]

VerPlank L, Li R. Cell cycle-regulated trafficking of Chs2 controls actomyosin ring stability during cytokinesis. Mol. Biol. Cell. 2005; 16:2529–2543. [PubMed: 15772160]

Verse1e M, Thorner J. Septin collar formation in budding yeast requires GTP binding and direct phosphorylation by the PAK, Cla4. J. Cell Biol. 2004; 164:701–715. [PubMed: 14993234]

Walther A, Wendland J. Septation and cytokinesis in fungi. Fungal Genet. Biol. 2003; 40:187–196. [PubMed: 14599886]

Watts FZ, Shiels G, Orr E. The yeast *MYO1* gene encoding a myosin-like protein required for cell division. EMBO J. 1987; 6:3499–3505. [PubMed: 3322809]

Weiss P, Huppert S, Kölling R. ESCRT-III protein Snn mediates high-level expression of the SUC2 gene via the Rim101 pathway. Eukaryot. Cell. 2008; 7:1888–1894. [PubMed: 18806212]

Wemmer M, Azmi I, West M, Davies B, Katzmann D, Odorizzi G. Brol binding to Snn regulates ESCRT-III membrane scission activity in yeast. J. Cell Biol. 2011; 192:295–306. [PubMed: 21263029]

Wollert T, Wunder C, Lippincott-Schwartz J, Hurley JH. Membrane scission by the ESCRT-III complex. Nature. 2009; 458:172–177. [PubMed: 19234443]

Xu X, Vogel BE. A secreted protein promotes cleavage furrow maturation during cytokinesis. Curr. Biol. 2011; 21:114–119. [PubMed: 21215633]

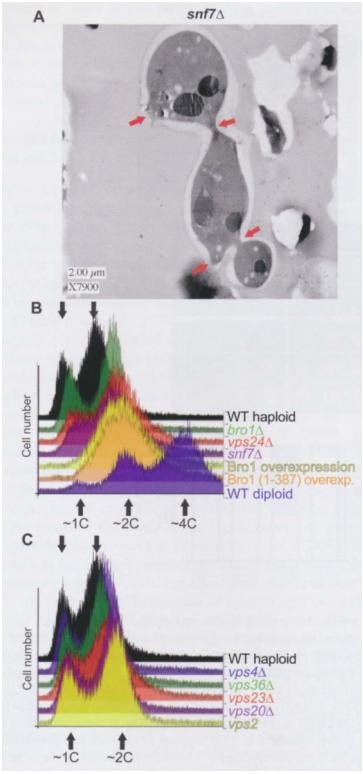

Figure 1.

Cytokinesis failure and aberrant DNA content in cells with ESCRT-III defects.

(A) High-pressure frozen and freeze-substituted cells of strain MWY24 were embedded in plastic, thin-sectioned and visualized by TEM. The red arrows indicate sites of impending or aborted cytokinesis. (B) Approximately 10 000 PI-stained cells of each indicate genotype were analyzed by flow cytometry to measure DNA content. Histograms of the resulting distributions were manually offset rightward on the *x*-axis to facilitate comparison of the profiles. The arrows indicate the approximate peak values corresponding to IC, 2C, or 4C DNA content. The strains were: SEY6210 (WT haploid), GOY65 (*brolΔ*), BWY102 (*vps24Δ*), MWY24 (*snf7Δ*), SEY6210 carrying plasmid pG0216 (Brol overexpression), SEY6210 carrying plasmid pMWM3 [Brol (1–387) overexpression], and SEY6210 diploid (WT diploid). (C) As in (B), for strains SEY6210 (WT haploid), MBY3 (*vps46Δ*), MBY30 (*vps36Δ*), EEY6-2 (*vps23Δ*), EEY2-1 (*vps20Δ*), and MBY28 (*vps2Δ*).

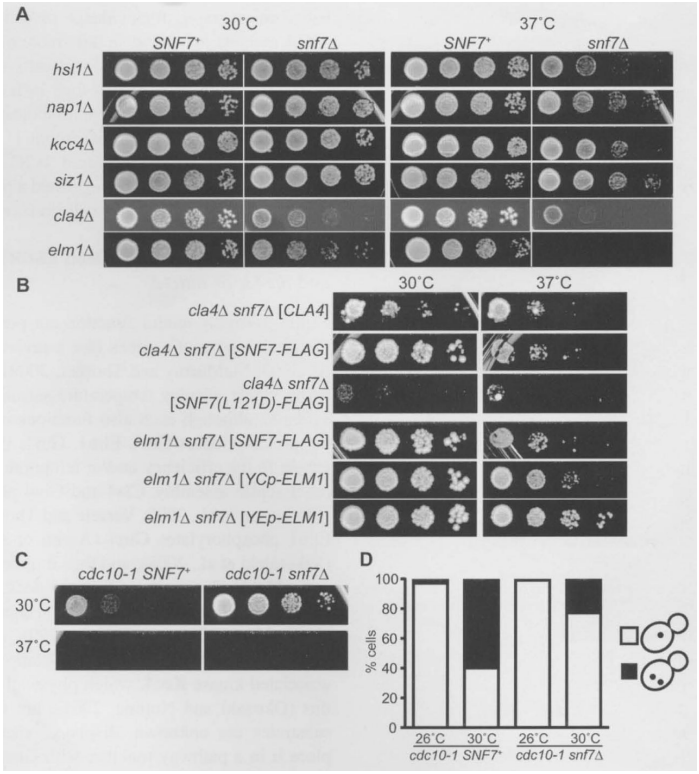

Figure 2.

Synthetic effects on colony growth and/or number of nuclei in *snf7Δ cla4Δ, snf7Δ elm1Δ*, and *snf7Δ cdc10-1* mutants.

(A–C) Fivefold serial dilutions of cells cultured at room temperature were spotted on agar plates and incubated at the indicated temperature for 2–3 d before plates were photographed. The growth medium was rich (YPD) (A, C), or synthetic drop-out medium selective for the indicated plasmids (B). All strains were, as indicated, the *SNF7*$^{+}$ or *snf7Δ* meiotic progeny of diploid cells carrying a mutation at another locus, and were made by crossing the *snf7Δ* haploid JTY4935 with JTY4003 (*hsl1Δ*), JTY4007 (*nap1*), JTY4005 (*kcc4Δ*), JTY4008 (*siz1Δ*), YMYB12 (*cla4Δ*), JTY4000 (*elm1Δ*), or JTY3986 (*cdc10-1*), Plasmids FD44 ([*CLA4*]), pRS416-*SNF7-FLAG* ([*SNF7-FLAG*]), pRS416-*SNF7 (L121D)-FLAG* ([*SNF7 (L121D)-FLAG*]), pRS416-CUP-*ELM1* ([*YCpELM1*]) or YEp13-*ELM1* ([YEp-*ELM1*]) were introduced by transformation into the haploid spore clones. (D) The strains in (C) were grown overnight in YPD medium at the indicated temperature prior to DAPI staining and visualization of nuclei in single focal planes, At 26°C, for *cdc10-1 SNF7*$^{+}$, 14/475 were multinucleate at 26°C, 223/373 at 30°C; for *cdc10-1 snf7Δ*, 6/746 were multinucleate at 26°C, 86/382 at 30°C.

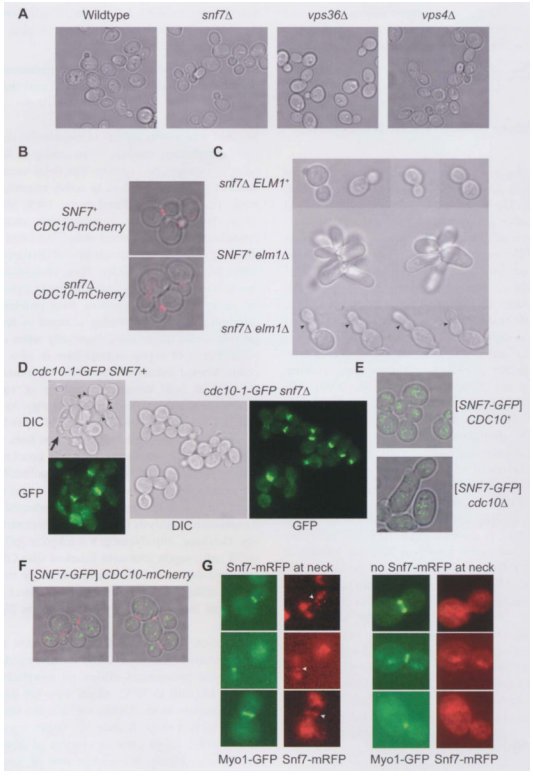

Figure 3.

ESCRT-III and septin localization patterns and effects on morphogenesis during normal and defective cell division.

Cells from exponentially-growing cultures were visualized by transmitted light microscopy of single focal planes (A–E) and either epifluorescence microscopy at regular intervals in the *z* direction combined with deconvolution of the resulting single focal plane images to eliminate out-of-plane fluorescence, followed by projection of each focal plane's image onto a single image (B, E), or standard epifluorescence microscopy of single focal planes (D, G). (A) Strains were SEY6210 (wild-type), MWY24 (*snf7Δ*), MBY30 (*vps36Δ*), or MBY3 (*vps4Δ*) and were cultured at 30°C. (B) mCherry-tagged Cdc10, expressed from the endogenous *CDCIO* locus, was visualized with a rhodamine filter set in *SNF7*$^{+}$ (JTY3992) or *snf7Δ* (YCS639) cells cultured at 30°C. (C) Cells of strain JTY4957 (*snf7Δ ELM1*), JTY4000 (*SNF7*$^{+}$ *elm1Δ*), or JTY4973 (*snf7Δ elm1Δ*) pre-grown in YPD at room temperature were shifted to 37°C for 3 h. The arrowheads indicate constrictions along the lengths of *snf7Δ elm1Δ* buds. (D) Cells of strain JTY3986 (*cdc10-1-GFP SNF7*$^{+}$) or JTY4000 (*cdc1O-1-GFP snf7Δ*), pre-grown in YPD at room temperature, were shifted to 30°C for 3 h. Cell morphology was visualized by differential interference contrast (DIC). Cdc10-1-GFP localization was visualized with an eGFP filter set (GFP). The arrowheads indicate cells with multiple attached buds. The arrow indicates an elongated, lysed cell. (E) Snf7-GFP was visualized with a TRITC filter set in cells of strain BY4741 (*CDC10*$^{+}$) or YCS640 (*cdc10Δ*) cultured at 30°C and carrying plasmid pRS416-*SNF7-GFP*. (F) Snf7-GFP (green) and Cdc10-mCherry (red) were visualized in cells of strain JTY3992 cultured at 30°C using a TRITC or a rhodamine filter set, respectively. (G) Snf7-mRFP (red) and Myol-GFP (green) were visualized using a TRITC or an eGFP filter set, respectively, in diploid cells made by mating strain JTY3562 with strain JTY4510 and cultured at 30°C. Left column: cells with Snf7-mRFP at the bud neck (arrowheads); right column: cells in which no Snf7-mRFP was observed at the neck, imaged in the same fields as those in the left column.

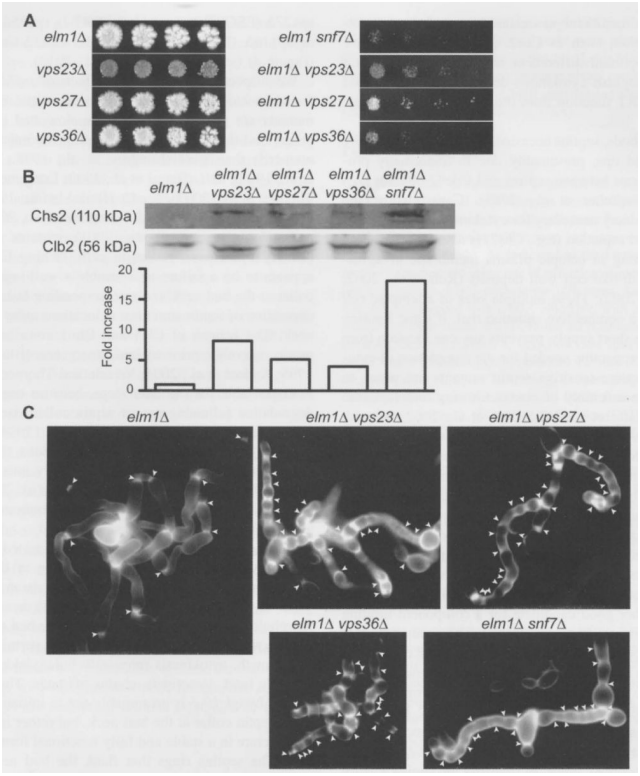

Figure 4.

ESCRT-I, -II, and -III mutations in *elm1Δ* cells exacerbate cytokinesis defects, elevate Chs2 levels, and cause ectopic chitin deposition.

(A) Fivefold serial dilutions of cells cultured at room temperature were spotted on a YPD agar plate and incubated at 37°C for 3 d before colonies were photographed. (B) Top: Immunoblot of Chs2 and Clb2 from protein extracts of the indicated strains. Bottom: the ratio of intensity of Chs2 to another loading control (Pgk1; not shown) for each lane above is plotted and normalized to the value for the *elm1Δ* strain JTY4000. (C) YPD cultures of the indicated strains were grown to saturation at room temperature and stained with the chitin-binding dye Calcofluor White. Chains of elongated cells were selected for imaging. Arrowheads: regions of intense staining. Strains were, as indicated, JTY4000 (*elm1Δ*), JTY5595 (*vps23Δ*), JTY5596 (*vps27Δ*), JTY5597 (*vps36Δ*), JTY4973 (*elmlΔ Snf7Δ*), JTY5598 (*elm1Δ vps23Δ*), JTYSS99 (*elm1Δ vps27Δ*), JTY5600 (*elm1Δ vps36Δ*).